Sensors & Transducers, Vol. 255, Issue 1, January 2022, pp. 35-43

Sensors & Transducers

Published by IFSA Publishing, S. L., 2022
http://www.sensorsportal.com

Lock-in Phenomena in a Ring Laser

*** Aleksei ZADVORKIN and Tatiana RADINA**
St. Petersburg State University, Ulyanovskaya 1, 198504, Petergof, St. Petersburg, Russia
* Tel.: +7-911-0314984
E-mail: zlelik2000@gmail.com

Received: 4 December 2021 /Accepted: 7 January 2022 /Published: 31 January 2022

Abstract: The problem of synchronizing counterpropagating waves in ring lasers is an integral part of the fundamental problem of synchronizing nonlinear oscillations. This phenomenon is inherent in all self-oscillating systems. As a continuation of the work [1] and extension of [2], an in-depth analysis of the obtained equations was performed for He Ne ring laser with an inhomogeneously broadened active medium. Alternative to backscattering explanation of the lock-in phenomena [3] was suggested and it is counterpropagating waves phase relationship through their nonlinear polarization. Comparative analysis of the behavior of frequencies and intensities for the single-mode ring laser working on a single isotope of Ne and on the mix of ^{20}Ne ^{22}Ne isotopes was conducted. Dependency of the lock-in threshold on different parameters including active medium pressure, cavity detuning, pumping current value, rotation speed, etc. were theoretically researched. The intensity of counterpropagating waves was analyzed. Theoretical predictions were compared with experimental data. The most important results are presented in this work.

Keywords: Ring laser, Nonlinear coupling, Frequency synchronization, Gyroscope.

1. Introduction

The creation of a ring laser has created a unique possibility for conducting precision research in various fields of fundamental physics. For example, the creation of detectors of gravitational waves [4], the study of relativistic and gravitational effects in the theory of relativity [5, 6] verification of the effects of quantum electrodynamics [4], and other phenomena [7]. One of the important applications of the ring laser is a laser gyroscope sensor. The accuracy of modern gyroscopes makes it possible to measure the unevenness of the Earth's rotation [7].

The principle of operation of this equipment is based on the Sagnac effect. Two counterpropagating waves in the ring laser have different frequencies if the propagation conditions of the waves are different. One of these conditions can be the rotation of the ring laser. Frequency differences can be easily measured by optical heterodyne detection.

Ring lasers are complex nonlinear self-oscillating systems with output characteristics, which (and, hence, the accuracy of measurements) are dependent on many factors. In essence, the problem of finding the frequencies and intensities of the generation of counterpropagating waves of the same mode is the problem of finding normal modes of an optical resonator with a nonlinear active medium. The presence of a nonlinear medium in the resonator dictates the use of the self-consistent method, first used by Lamb [8] for the construction of laser theory.

The obtained results, for the first time, made it possible to explain the behavior of the frequency differences and intensities of laser generation in single-mode gas laser operating on pure isotope, in the entire generation region (including the region of strong coupling). In addition, they made it possible to systematize the experimental data accumulated in the course of many years of research, to establish the regularities of the redistribution of the intensities of the generation of counterpropagating waves depending on the parameters of the resonator and the active medium.

During the rotation of the laser gyroscope at a speed less than a certain critical value (called the lock-in threshold), the frequency difference of counterpropagating waves is insignificant, and reciprocal frequency synchronization is observed [9], which leads to the insensitivity of the laser gyroscope in a certain region of low rotation speeds, where the beat frequency becomes equal to zero. A large number of works [9 - 10] are devoted to the study of the synchronization phenomenon in ring gas lasers. The main, and often the single reason for the reciprocal frequency synchronization is considered to be the coupling of waves through backscattering when part of the field of one wave is scattered by a single inhomogeneity in the direction of the other. This model does not find sufficient physical justification.

In the work [1], another, fundamentally unavoidable, reason for the coupling of counterpropagating waves was proposed. This is a phase relationship through their nonlinear polarization. More precisely, through that component of polarization, the origin of which is caused by the modulation of the population difference between the energy levels with frequency $\omega_r - \omega_l$. Where ω_r is the frequency of the right wave and ω_l is the frequency of the left wave. We note that the modulation of the population difference is the reason for the existence of the strong-coupling region.

This work is an extension of [1]. Here we conducted a comparative analysis of the behavior of frequencies and intensities of single-mode lasers operating on pure isotope Ne and the mixture ^{20}Ne ^{22}Ne isotopes. Note that the transition to a two isotopic medium does not affect the general form of the laser equations. Only the expressions for the polarization coefficients change.

2. Main Equations

The self-consistent problem of an optical ring resonator with a nonlinear active medium was solved. The electric field of counterpropagating waves ($j = r, l$) is defined as:

$$E_j(z,t) = E_{0j} exp\left\{\pm ik\int_0^z n_j(\tilde{z})d\tilde{z} - i\omega t \mp \frac{\varphi(t)}{2}\right\}, \quad (1)$$

where $\frac{\varphi(t)}{2}$ are the phase shifts of each wave caused by rotation.

The complex refractive index $n_j(z) = n_j'(z) + in_j''(z)$ of a nonlinear medium is induced by the interaction of counterpropagating waves in the active medium. $n_j(z)$ was found via polarization by a quantum mechanical method suggest by Lamb [8]. Unlike [8] and other authors, all calculation was performed in complex variables, in the analytical form in the third-order of the perturbation theory with the weak-field limit without additional approximations.

The final system of the equations is obtained from the periodicity conditions which are necessary for the existence of stationary generation in the resonator:

$$\eta_r = \beta_r'' I_r + \theta_l'' I_l + (\sigma_r'' cos\varphi - \sigma_r' sin\varphi)\sqrt{I_r I_l}, \quad (2)$$

$$\eta_l = \beta_l'' I_l + \theta_r'' I_r + (\sigma_l'' cos\varphi + \sigma_l' sin\varphi)\sqrt{I_r I_l}, \quad (3)$$

$$\dot{\varphi} = \Delta\omega - \frac{c}{L}KH\{2 \vartriangle Z' - I_r(\beta_r' - \theta_r') + I_l(\beta_l' - \theta_l') - 2(\vartriangle \sigma' cos\varphi - \sigma'' sin\varphi)\sqrt{I_r I_l}\}, \quad (4)$$

where $I_{r,l}$ is the dimensionless intensities, $\eta_j = Z_j'' - \frac{\varepsilon_j}{KH}$, $\beta_{r,l}$, $\theta_{r,l}$ are the polarization coefficient of self-saturation and cross-saturation respectively of right and left waves, Z' is the linear dispersion, Z' is the coefficient of linear gain, KH is the gain on the length of the tube H. The phase coupling of counterpropagating waves is caused by the parametric effects (polarization terms proportional to $\sigma_{r,l}'', \sigma_{r,l}'$) in a nonlinear active medium. The interaction of counterpropagating waves is carried out in a nonlinear active medium.

Imaginary and real parts of the $\beta_{r,l}$, $\theta_{r,l}$, Z $\sigma_{r,l}$ are shown in the Fig. 1 and Fig. 2 below.

Polarization coefficient σ, which is the only reason for frequency synchronization is 5 orders of magnitude smaller than other polarization coefficients ($\beta_{r,l}$, $\theta_{r,l}$, Z). This insignificant value is enough to change the behavior of the frequencies of counterpropagating waves and introduce lock-in phenomena.

Solving system (2) - (4) gives classical Adler's equation.

$$\dot{\varphi} = \Delta\widetilde{\omega} - Bsin\varphi \quad (5)$$

It can be used to derive boundaries of the lock-in range and the expressions for intensities:

$$\Delta\omega_d - B < \dot{\varphi} < \Delta\omega_d + B, \quad (6)$$

where

$$B = \frac{c}{L}\frac{2(KHZ'' - \varepsilon)}{\beta'' + \theta''}\left\{\sigma'' - \sigma'\frac{\beta' - \theta'}{\beta'' - \theta''}\right\} \quad (7)$$

$$\Delta\widetilde{\omega} = \Delta\omega + \Delta\omega_d, \Delta\omega_d = 2\Delta\varepsilon\frac{c}{L}\frac{\beta' - \theta'}{\beta'' - \theta''} \quad (8)$$

Here $\Delta\omega_d$ is the laser gyroscope null shift caused by a nonreciprocal element.

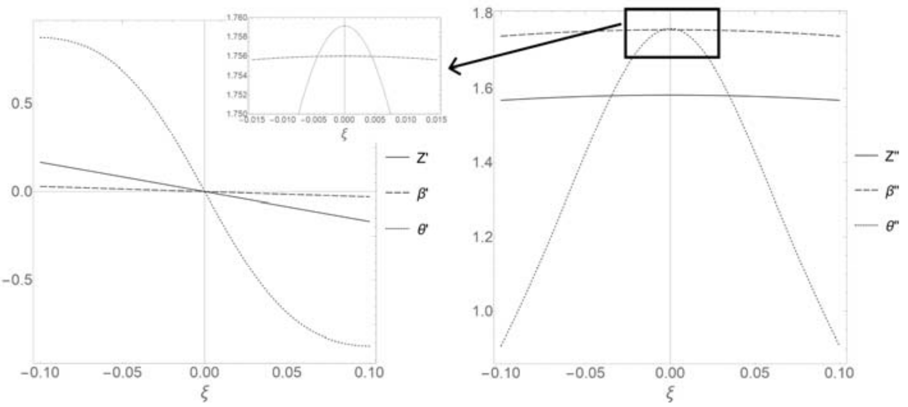

Fig. 1. Real part (on the left) and imaginary part (on the right) of polarization coefficients β, θ and Z depending on the relative detuning for zero frequency difference between counterpropagating waves and single isotope active medium.

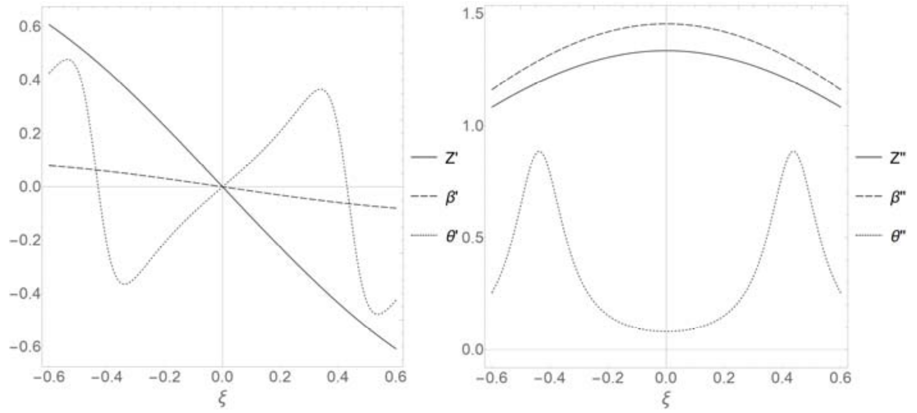

Fig. 2. Real part (on the left) and imaginary part (on the right) of polarization coefficients β, θ and Z depending on the relative detuning for zero frequency difference between counterpropagating waves and 50 % mixture of ^{20}Ne, ^{22}Ne isotopes active medium.

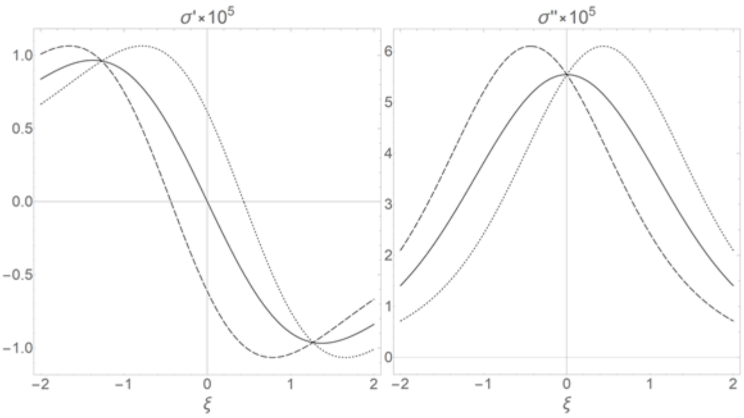

Fig. 3. Real part (on the left) and imaginary part (on the right) of polarization coefficient σ depending on the relative detuning for zero frequency difference between counterpropagating waves. Dashed lines are for single isotope and solid line for 50 % mixture of ^{20}Ne, ^{22}Ne isotopes active medium.

Intensities can be derived in the approximation $\Delta I \ll I$ using the notation $2I = I_r + I_l$, $2\Delta I = I_r - I_l$. In this case, $\Delta I / I$ can be neglected and the expression $\sqrt{I_r I_l}$ can be simplified as $\sqrt{I_r I_l} = I$.

$$I_{r,l} = I \pm \Delta I \tag{9}$$

$$I = \frac{\eta}{\beta'' + \theta''} \tag{10}$$

$$\Delta I = \frac{1}{\beta'' - \theta''}\left\{\Delta\eta + \eta\frac{\sigma' sin\varphi}{\beta'' + \theta''}\right\} \tag{11}$$

3. Discussion of the Numerical Calculation Results

Lock-in boundaries and intensity were researched theoretically based on Eqs. (2) - (4) for the wide range of ring laser configuration such as single isotope and mixture of ^{20}Ne, ^{22}Ne isotopes and by varying a significant number of different parameters including pressure in the active medium, gain value, detuning, resonator rotation speed, same and different losses for counterpropagating waves, etc. Based on Eqs. (9) - (11) calculations of intensities and additional frequencies difference were performed. The results for a single isotope and different losses or frequency difference are presented in Fig. 4, Fig. 5.

In case when frequency difference and different losses for counterpropagating waves are presented at the same time, the function of intensities becomes asymmetric. This special situation is presented in Fig. 6 and was noted in many experimental works.

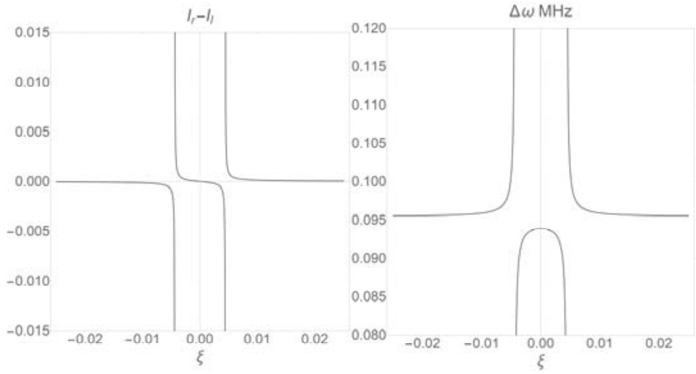

Fig. 4. Intensities difference for counterpropagating waves $I_r - I_l$ on the left and additional frequency difference for counterpropagating waves $\omega_r - \omega_l$ on the right depending on the relative detuning for non-zero frequency difference $\Delta\omega = 0.106\ MHz$, $\varepsilon_r = \varepsilon_l = 0.1$, $KH = 0.12$ and single isotope active medium.

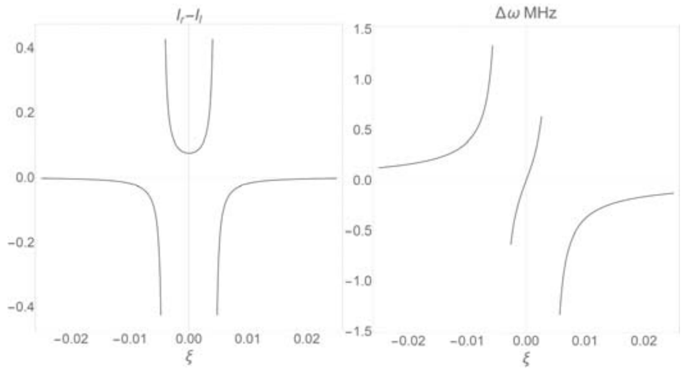

Fig. 5. Intensities difference for counterpropagating waves $I_r - I_l$ on the left and additional frequency difference for counterpropagating waves $\omega_r - \omega_l$ on the right depending on the relative detuning for different losses and zero frequency difference $\Delta\omega = 0\ MHz$, $\varepsilon_r = 0.1$, $\varepsilon_l = 0.1001$, $KH = 0.12$ and single isotope active medium.

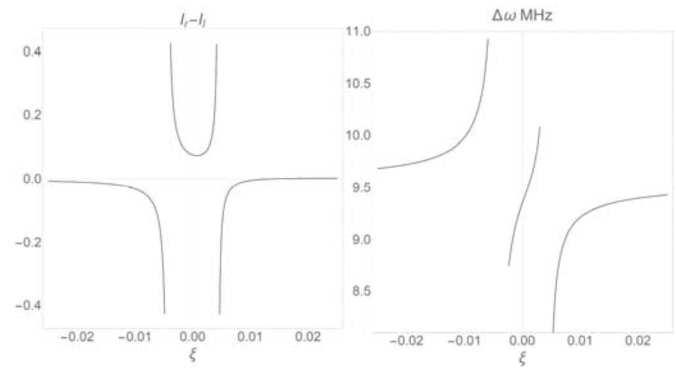

Fig. 6. Intensities difference for counterpropagating waves $I_r - I_l$ on the left and additional frequency difference for counterpropagating waves $\omega_r - \omega_l$ on the right depending on the relative detuning for different losses and none-zero frequency difference $\Delta\omega = 10.6\ MHz$, $\varepsilon_r = 0.1$, $\varepsilon_l = 0.1001$, $KH = 0.12$ and single isotope active medium.

The results for a mixture of ^{20}Ne, ^{22}Ne isotopes can be found in Fig. 7, Fig. 8. Similar to a single isotope active medium, for simultaneous presence of frequency difference and different losses for counterpropagating waves, functions of intensity and frequency difference become asymmetric as shown in Fig. 9.

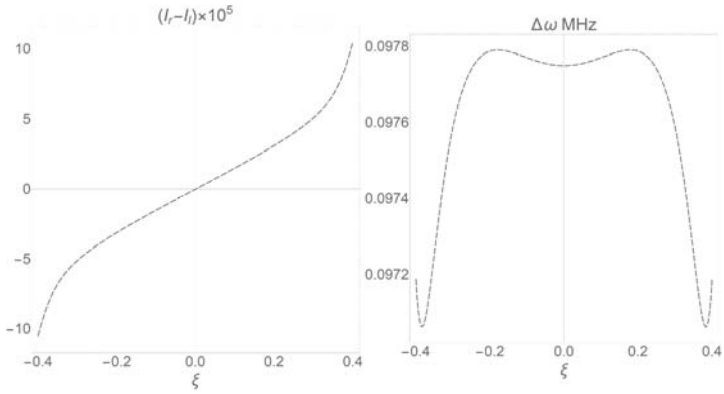

Fig. 7. Intensities difference for counterpropagating waves $I_r - I_l$ on the left and additional frequency difference for counterpropagating waves $\omega_r - \omega_l$ on the right depending on the relative detuning for non-zero frequency difference for $\Delta\omega = 0.106\ MHz$, $\varepsilon_r = \varepsilon_l = 0.1$, $KH = 0.12$ and 50 % mixture of ^{20}Ne, ^{22}Ne isotopes active medium.

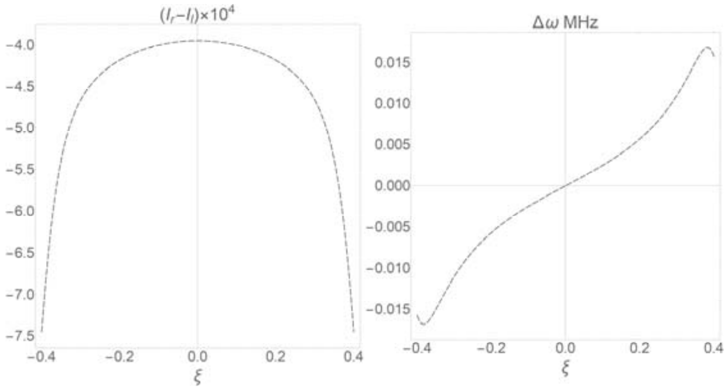

Fig. 8. Intensities difference for counterpropagating waves $I_r - I_l$ on the left and additional frequency difference for counterpropagating waves $\omega_r - \omega_l$ on the right depending on the relative detuning for different losses and zero frequency difference for $\Delta\omega = 0\ MHz$, $\varepsilon_r = 0.1$, $\varepsilon_l = 0.1001$, $KH = 0.12$ and 50 % mixture of ^{20}Ne, ^{22}Ne isotopes active medium.

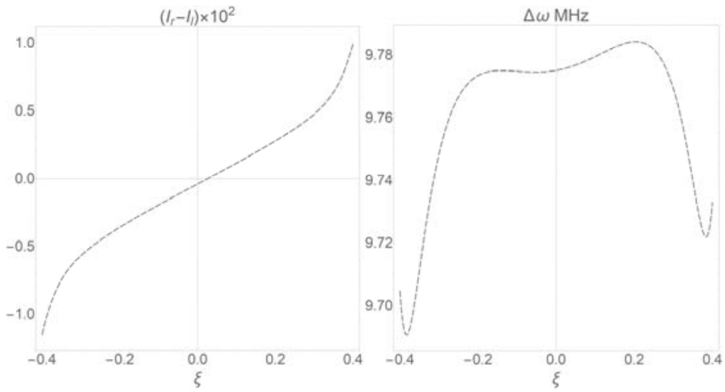

Fig. 9. Intensities difference for counterpropagating waves $I_r - I_l$ on the left and additional frequency difference for counterpropagating waves $\omega_r - \omega_l$ on the right depending on the relative detuning for different losses and non-zero frequency difference for $\Delta\omega = 10.6\ MHz$, $\varepsilon_r = 0.1$, $\varepsilon_l = 0.1001$, $KH = 0.12$ and 50 % mixture of ^{20}Ne, ^{22}Ne isotopes active medium.

As shown in Fig. 4 for a single isotope active medium there is an area of strong coupling of the waves. In this range of relative detuning, energy is redistributed between the weak and the strong waves and intensities for counterpropagating waves have corresponding peaks. However, the total intensity does not have these peaks. In addition, it was noted, that in the middle of the gain curve ΔI is zero.

Analysis of Eq. (11) for intensities difference inside lock-in range ($\Delta\omega = 0$) shows that ΔI is an odd function due to the fact that σ' is an odd function. Outside lock-in range ΔI is the odd function as well. ΔI close to the center of the gain curve has the same behavior inside and outside lock-in range as shown in Fig. 4 and Fig. 10. The detailed research of the behavior of σ' and σ'' was conducted in [1] and in Fig. 3 of that work. The presence of $sin\varphi$ in the Eq. (11) explains the intensity oscillations reported in [11] and other experimental works, which could not be theoretically justified before.

B in Eq. (7) makes the main contribution into synchronization threshold as follows from (5). As shown in Fig. 11, B is an even function because functions $Z'', \beta'', \theta'', \sigma''$ in Eq. (7) are even functions. The evenness of $Z'', \beta'', \theta'', \sigma''$ was discussed in [1] and shown in Fig. 1 and Fig. 2. B has a maximum on the center of the gain curve.

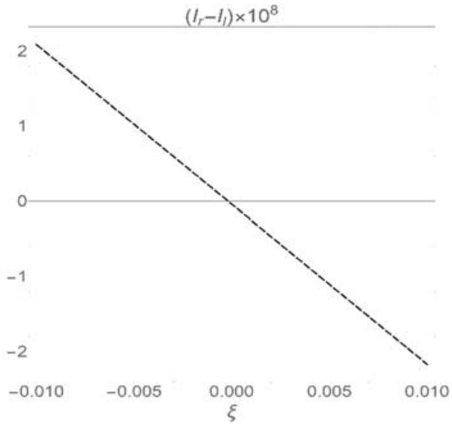

Fig. 10. Intensities difference for counterpropagating waves $I_r - I_l$ on the relative detuning inside lock-in region for $\Delta\omega = 0$, $\varepsilon_r = \varepsilon_l = 0.1$, $KH = 0.12$ and 50 % mixture of ^{20}Ne, ^{22}Ne isotopes active medium.

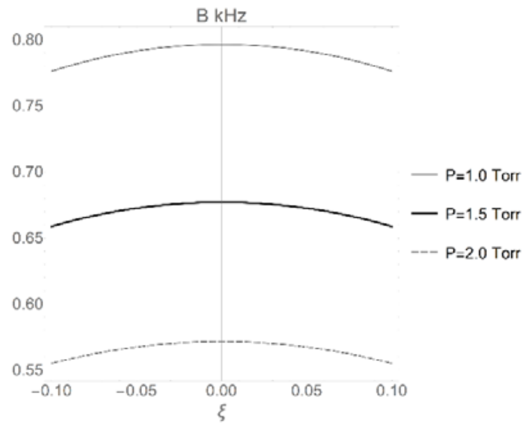

Fig. 11. Dependency of parameter $\boldsymbol{B}$ on the relative detuning for different pressure in the active medium for $\boldsymbol{\varepsilon_r = \varepsilon_l = 0.1}$, $\boldsymbol{KH = 0.12}$ and 50 % mixture of ^{20}Ne, ^{22}Ne isotopes active medium.

Fig. 12 shows the calculations of the intensity depending on resonator rotation speed for different gain. The lines for intensities on Fig. 12 are interrupted at the point of the lock-in threshold, which means the lock-in threshold is increasing with the increase of active medium gain. The explanation can be given from the fact, that frequency synchronization is a non-linear effect and nonlinearity increases with the increase of the active medium gain. On another side, as shown in Fig. 11, the lock-in threshold decreases with increasing of the active medium pressure. This is due to the raise of the relaxation constants with the pressure growths. It can be noted that frequency synchronization effect is complex, nonlinear effect and many different parameters can influence lock-in threshold, such as active medium pressure, gain, pumping current, etc.

Calculations for Fig. 12 were carried out under the condition that the gain K remains unchanged over the cross-section of the tube. However, in the experiments, the transverse distribution of the gain changes significantly with the increasing of the pumping current as shown in Fig. 13. This effect can lead to the reduction of the active medium gain with the increasing of pumping current due to the dependency of relaxation constants on this current. In our opinion, that is the reason for the deviation of Fig. 12 and similar figures in [3].

β_j, θ_j and respectively synchronization threshold depend on the active medium pressure and gain, relative detuning, and other parameters. Fig. 14 is an example of such dependency.

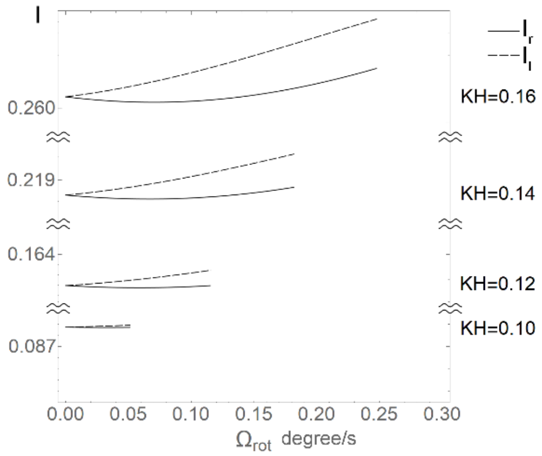

Fig. 12. Dependencies of intensities for counterpropagating waves on the speed of resonator rotation for various values of KH.

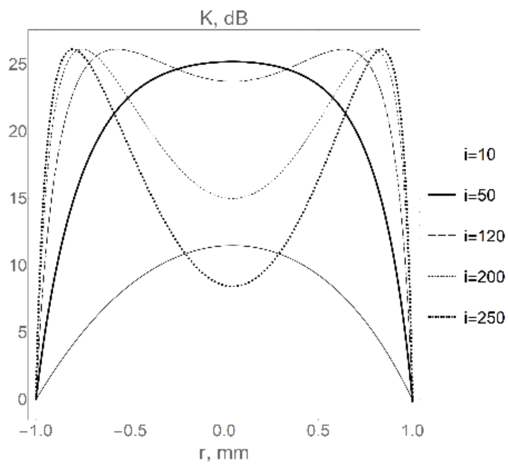

Fig. 13. Transverse distribution of the gain $\boldsymbol{K}$ for different pumping currents in mA.

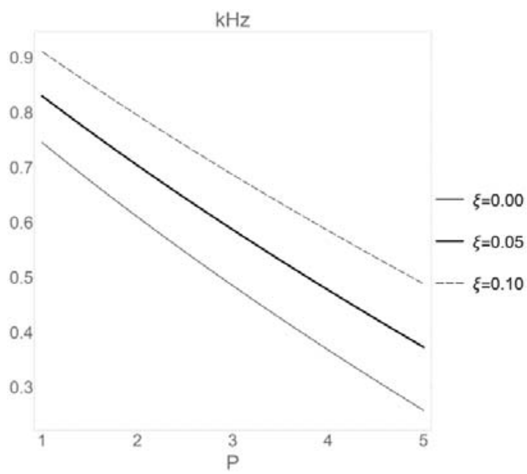

Fig. 14. Dependences of the synchronization threshold on the pressure (Torr) at various relative detuning.

4. Conclusions

Detailed analysis of the results of work [1] was conducted. Synchronization in ring lasers is a multiparametric frequency-dependent effect and depends on the design and geometry of the cavity, as well as on the pumping current, pressure in the active medium, cavity rotation speed, etc. To understand the specifics of the laser work, in every case, it is necessary to have a detailed understanding of the configuration of the laser.

Intensities of counterpropagating waves were researched depending on different laser parameters such as relative detuning, single isotope and isotopes mixture, different losses and frequencies differences of counterpropagating waves. The results for intensities are presented. Qualitative behavior of intensities difference retains the same inside and outside lock-in range boundaries. For the first time, the oscillations in the intensities obtained in [11] were theoretically explained.

It was established theoretically, that lock-in range boundaries are decreasing when pressure is increasing. As a result of the research of Eq. (8), it was confirmed theoretically that the synchronization threshold is higher when the active medium gain is higher and adding a second isotope to the active medium is decreasing the lock-in threshold. In addition, increasing of synchronization threshold while increasing detuning was also predicted based on equations analysis. Comparison with experimental data was conducted. For comparison with the experiment, it is necessary to take into account the change in the spatial distribution of the gain over the cross-section of the tube with the active medium.

5. Annex A. Expressions for Polarization Coefficients

In this Annex full expressions for polarization coefficients $\beta_{r,l}$, $\theta_{r,l}$, Z, $\sigma_{r,l}$ are given.

Polarization calculation from the system of equations for the elements of the density matrix in the third order of the perturbation theory was performed in many works [8], [12] where a small parameter is given by:

$$I_j = \frac{|dE_j|^2}{\hbar}\frac{1}{\gamma_{ab}}\left(\frac{1}{\gamma_a}+\frac{1}{\gamma_b}\right), \tag{12}$$

where d is the transition dipole moment. The fact that this small parameter is proportional to $|E_j|^2$, allows to call it dimensionless intensity of the wave.

Unlike other authors Lamb and others we did not separate equations to real and imaginary part. This approach gave a possibility to find analytical equations for polarization coefficients without additional approximations. The detailed description can be found in [13]. Polarization of j -wave is represented in the following form

$$\begin{aligned}2\pi\kappa_j(\mathrm{z}) = (1/k)K\Big\{&Z_j - \beta_j I_j - \theta_{j'} I_{j'} \\ &- \sigma_j\sqrt{I_j I_{j'}}exp\{\mp i\varphi\}\Big\}\end{aligned} \tag{13}$$

Here it was taken into account the following

$$\begin{aligned} &E_r(z)E_l^*(L-z) \\ &= E_{0r}E_{0l}exp\left\{ik\int_0^z n_j d\tilde{z}\right\} \\ &\times exp\left\{-ik\int_0^{L-z} n_j d\tilde{z}\right\}^* \\ &= E_{0r}E_{0l}exp\left\{i\frac{2\pi}{\lambda}L\right\} \\ &\times exp\left\{-k\int_0^L (n_j'')d\tilde{z}\right\} \\ &= E_{0r}E_{0l}exp\{\pm i2\pi q\}exp\{-kHn_j''\} \\ &= E_{0r}E_{0l}exp\{-kHn_j''\}\end{aligned} \tag{14}$$

$K = 2\pi d^2N/(\hbar u)$ – gain coefficient per unit length, N – excitation density, u – root mean square velocity of the active medium atoms.

Expression for Z function, which real part describes the linear dispersion (Z') and imaginary part linear amplification (Z'') of the active medium is given by (15).

$$Z(\zeta_j) = 2i\int_0^\infty exp\{-\rho^2 + 2i\rho\zeta_j\}d\rho, \tag{15}$$

where:

$\zeta_j = \frac{(\omega_j - \omega_{ab} + i\gamma_{ab})}{(ku)}$,

ω_{ab} is the frequency of the middle of the gain curve;

ku is the Doppler broadening;

γ_{ab} is the half-widths of the homogeneous line.

Polarization coefficient of self-saturation $\beta_{r,l}$ can be calculated by the following formula:

$$\beta_j = iZ_j'' + 2i\frac{\gamma_{ab}}{ku}\left(1+\zeta_j Z_j\right) \tag{16}$$

Cross-saturation coefficient $\theta_{r,l}$ can be represented as:

$$\theta_{j'} = \sum_{t=1}^{3}\theta_{j't} \tag{17}$$

$\theta_{r,l}$ is defined by two processes. First is saturation of population difference of the energy states, which leads to existence of the following two terms:

$$\begin{aligned}\theta_{j'1} = \frac{1+i\Delta}{2(1+\Delta^2)}&\left(Z_j + Z_{j'}\right) \\ &- \left(\frac{i}{2\Delta}\right)\left(Z_j + Z_{j'}^*\right)\end{aligned} \tag{18}$$

Last two terms in (17) appears due to parametric process of modulation of energy state population difference with frequency $\omega_j - \omega_{j'}$. Which leads to increase of the coupling of the counterpropagating waves.

$$\theta_{j'2} = f(\gamma/\gamma_{ab}) \sum_{n=a,b} |\nu_n|^{-2} \left\{ Z\left(\zeta_{jj'}^{(n)}\right) - \left(Z_j - Z_{j'}^*\right)/2 - \alpha_n \theta_{j'2} \right\}, \tag{19}$$

$$\theta_{j'3} = f(\gamma/\gamma_{ab}) \sum_{n=a,b} \nu_n^{-2} \left\{ Z_j \left(1 + 2\left(\gamma_{ab}/(ku)\right)^2 \nu_n \nu\right) - Z\left(\zeta_{jj'}^{(n)}\right) + \frac{2\nu_n\gamma_{ab}}{(ku)}, \right\} \tag{20}$$

$$\Delta = \frac{(\omega + \omega_{ab})}{\gamma_{ab}}, \omega = \frac{(\omega_j + \omega_{j'})}{2}, \tag{21}$$

$$\zeta_{jj'}^{(n)} = (\omega_j - \omega_{j'} + i\gamma_n)/(2ku), \tag{22}$$

$$\nu = \Delta + i, \nu_n = \Delta + i\alpha_n, \alpha_n = 1 - \frac{\gamma_n}{(2\gamma_{ab})}, \tag{23}$$

$$f = \gamma_a\gamma_b/(4\gamma^2), \gamma = (\gamma_a + \gamma_b)/2 \tag{24}$$

Modulation of the population difference of energy state is the main reason for the polarization terms proportional to $\sigma''_{r,l}, \sigma'_{r,l}$. Polarization coefficient σ_j has the form:

$$\sigma_j = \frac{\gamma_a\gamma_b}{8\gamma\gamma_{ab}} \sum_{n=a,b} \left\{ \frac{1}{\nu_{2n}} \left[\frac{3(\Delta - 2i)}{\nu_1\nu_2} Z\left(\frac{1}{3}\left(\zeta_j + \zeta_{jj'}\right)\right) + \frac{2i\alpha_{1n}}{|\nu_{1n}|^2} Z_{jj'}^{(n)} \right] - \frac{1}{\nu_1\nu_{1n}} Z_j + \frac{1}{\nu_2\nu_{1n}^*} Z_{j'}^* \right\}, \tag{25}$$

$$\nu_2 = 2\Delta - i, \nu_{2a,b} = \Delta + i\alpha_{2a,b}, \tag{26}$$

$$\alpha_{2a,b} = 1 - 3\gamma_{a,b}/(2\gamma_{ab}) \tag{27}$$

References

[1]. T. V Radina, Theory of frequency synchronization in a ring laser, *Physics Letters A*, Vol. 379, Issue 36, 2015, pp. 2140–2146.

[2]. A. Zadvorkin, T. Radina, Frequency synchronization in a ring laser, in *Proceedings of the 4th International Conference on Optics, Photonics and Lasers (OPAL'2021)*, 13-15 October 2021, Corfu, Greece, pp. 130–133.

[3]. B. Stieler, D. Loukianov, R. Rodloff, H. Sorg, Optical Gyros and their Application, D. Loukianov and North Atlantic Treaty Organization, *North Atlantic Treaty Organization, Research and Technology Organization*, 1999.

[4]. G. E. Stedman, Z. Li, C. H. Rowe, A. D. McGregor, H. R. Bilger, Harmonic analysis in a large ring laser with backscatter-induced pulling, *Physical Review A*, Vol. 51, Issue 6, 1995, pp. 4944–4958.

[5]. G. E. Stedman, H. R. Bilger, M. T. Johnsson, Z. Li, C. H. Rowe, T violation and microhertz resolution in a ring laser, *Optics Letters*, Vol. 20, Issue 3, 1995, pp. 324-326.

[6]. K. U. Schreiber, J.-P. R. Wells, Invited Review Article: Large ring lasers for rotation sensing, *Review of Scientific Instruments*, Vol. 84, Issue 4, 2013, p. 041101.

[7]. V. A. Alekseev, B. Y. Zel'dovich, I. I. Sobel'man, Parity non-conservation effects in atoms, *Uspekhi Fizicheskih Nauk*, Vol. 118, Issue 3, 1976, pp. 385-408.

[8]. W. E. Lamb, Theory of an Optical Maser, *Physical Review*, Vol. 134, Issue 6A, 1964, pp. A1429–A1450.

[9]. W. M. Macek, D. T. M. Davis, Rotation Rate Sensing with Traveling-Wave Ring Lasers, *Applied Physics Letters*, Vol. 2, Issue 3, 1963, pp. 67–68.

[10]. F. Bretenaker, B. Lépine, A. Le Calvez, O. Adam, J.-P. Taché, A. Le Floch, Resonant diffraction mechanism, nonreciprocity, and lock-in in the ring-laser gyroscope, *Physical Review A*, Vol. 47, Issue 1, 1993, pp. 543–551.

[11]. F. Aronowitz, R. J. Collins, Lock-In and Intensity-Phase Interaction in the Ring Laser, *Journal of Applied Physics*, Vol. 41, Issue 1, 1970, pp. 130–141.

[12]. F. Aronowitz, Theory of a Traveling-Wave Optical Maser, *Physical Review*, Vol. 139, Issue 3A, 1965, pp. A635–A646.

[13]. T. V. Radina, Diffraction phenomena in ring gas lasers, *Quantum Electronics*, Vol. 37, Issue 6, 2007, pp. 503–521.

___

Published by International Frequency Sensor Association (IFSA) Publishing, S. L., 2022 (http://www.sensorsportal.com).